Available online at www.sciencedirect.com
SCIENCE DIRECT®
Polymer 44 (2003) 3407–3415
polymer
www.elsevier.com/locate/polymer

Thermotropic liquid crystalline polymer (Rodrun LC5000)/polypropylene in situ composite films: rheology, morphology, molecular orientation and tensile properties

Sayant Saengsuwan[a,b], Sauvarop Bualek-Limcharoen[a,*], Geoffrey R. Mitchell[b], Robert H. Olley[b]

[a]*Department of Chemistry, Faculty of Science, Mahidol University, Rama 6 Road, Bangkok 10400, Thailand*
[b]*J.J. Thomson Physical Laboratory, Department of Physics, University of Reading, Reading RG6 6AF, UK*

Received 14 November 2002; received in revised form 3 February 2003; accepted 26 February 2003

Abstract

In situ composite films were prepared by a two-step method. First, polypropylene and thermotropic liquid crystalline polymer (TLCP), Rodrun LC5000 (80 mol% *p*-hydroxy benzoic acid (HBA)/20 mol% polyethylene terephthalate (PET)), were melt blended in a twin-screw extruder and then fabricated by extrusion through a mini-extruder as cast film. Rheological behavior of the blends, morphology of the extruded strands and films, and tensile properties of the in situ composite films were investigated. Rheological behavior of the blends at 295 °C studied using a plate-and-plate rheometer revealed a substantial reduction of the complex viscosity with increasing TLCP content, and all specimens exhibited shear thinning behavior. Over the angular frequency range of 0.6–200 rad/s, the viscosity ratio (dispersed phase to matrix phase) was found to be very low, in the range of 0.03–0.07. Morphologies of the fracture surfaces of the blend extrudates and the film surfaces etched in permanganic solution were investigated by scanning electron microscope (SEM). The TLCP droplets in the extruded strands were seen with a progressive deformation into fibrillar structure when TLCP content was increased up to 30 wt%. In the extruded films, TLCP fibrils with increasing aspect ratio (length to width) were observed with increasing TLCP concentration. Orientation functions of each component were determined by X-ray diffraction using a novel separation technique. It was observed that the Young's modulus in machine direction of the extruded film was greatly improved with increasing TLCP loading, due to the increase in fiber aspect ratio and also molecular orientation.

Keywords: In situ composite films; Rodrun LC5000; Polypropylene

1. Introduction

Thermotropic liquid crystalline polymers (TLCPs) blended with various kinds of thermoplastics (TPs) have been extensively studied since the late 1980s [1–4]. Most TLCP/TP blends are immiscible, with the dispersed TLCP phase in the form of droplets which can be deformed into fibers and oriented along the flow direction by shear or/and elongational force during melt processing. Rapid solidification ensures that these fibers are retained in an extended form in the matrix and hence reinforced it in a similar manner as a conventional short fiber-reinforced composites; these systems have been called 'in situ composites' [1]. It has also been found that the addition of a small amount of TLCP to a TP resulted in a reduction of the melt viscosity and thus acted as a processing aid with subsequent reduction of wear in processing equipment [5,6]. The mechanical properties of the resultant in situ composites are controlled by their morphology, which in turn depends on the rheological properties of the blend and its components, such as the viscosity ratio and the interfacial tension [7–9]. A requirement for the deformation of polymer dispersed droplets in the molten state is that the viscosity ratio (dispersed phase to matrix) should be less than unity [10]. Fibrillar structures were reported in some blend systems with the viscosity ratios far below 0.1 [11–14]. In situ composites fabricated by different methods, such as injection molding, compression molding, extruded sheet, fiber spinning and film extrusion [8,15], resulted in different morphology and degree of orientation. As a consequence, their mechanical properties are different. For thick products, a skin-core effect could be observed in that oriented fibrils were exhibited near to the skin of the molded part while

* Corresponding author. Tel.: +662-2015164; fax: +662-2458332.
E-mail address: scsbl@mahidol.ac.th (S. Bualek-Limcharoen).

0032-3861/03/$ - see front matter © 2003 Elsevier Science Ltd. All rights reserved.
doi:10.1016/S0032-3861(03)00244-1

TLCP droplets were present in the core region [16]. Although specimens prepared as films [17,18], showed minimal skin-core effect the properties measured in machine (MD) and transverse directions (TD) were significantly different. This problem could be overcome through the use of a counter-rotating die for thin film extrusion [19].

Polyolefins, such as polyethylene (PE) and polypropylene (PP) are interesting to use as the matrix for in situ composites because of their several excellent properties coupled with a low price. Recently, Bualek-Limcharoen et al. have studied the composite films of various grades of PP [12] and low density PE [14] blended with Rodrun LC3000 (a copolyester of 60 mol% *p*-hydroxy benzoic acid (HBA)/20 mol% polyethylene terephthalate (PET), emphasizing the effect of processing conditions, viscosity ratio and compatibilizers on the blend rheology, morphology and mechanical properties. We found that the mechanical properties, especially in the MD direction and impact strength of the films can be significantly improved by incorporation of TLCP together with a small amount of styrene based TP elastomer as compatibilizer. Though, various kinds of TLCPs, such as Vectra A (a copolyester of hydroxy naphthoic acid and hydroxyl benzoic acid), Vectra B (a copolyesteramide of hydroxy naphthoic acid, terephthalic acid and aminophehol) and Rodrun LC3000 have been used to blend with PP [8,12,20]. Only few groups have investigated the properties of LC5000/PP blend systems [21,22], Xu et al. [21] prepared 30 wt% LC5000/PP in situ composite by using injection molding and observed a ribbon-like structure. They also added polycarbonate and maleic anhydride grafted PP as a third component in order to improve the morphology and increase the strength and toughness of the composites. Sukananta et al. [22] studied the properties of as-spun and drawn monofilaments of LC5000/PP in situ composite, and found the significant improvement of both tensile and dynamic mechanical properties, especially in the high temperature region.

In the present work, in situ composite films were prepared from PP with varying amounts of TLCP (Rodrun LC5000) by using a two-step method. In the first step, the polymers were melt blended in a twin-screw extruder to get appropriate dispersion of TLCP phase. In the second step, the blend pellets were fabricated as extruded film using a mini-extruder equipped with a cast film line. Here we relate the resultant morphologies, characterized using electron microscopy and wide-angle X-ray scattering procedures to the mechanical properties of the PP/LC5000 in situ composite films.

2. Experimental

2.1. Materials

Polypropylene (PP), trade name PRO-FAX 6631 with melt flow index 2 g/10 min and a density of 0.903 g cm^{-3}, kindly provided by HMC Co., Thailand, was used as a matrix phase. The melting point of PP is about 165 °C. The reinforcing component was a semi-flexible thermotropic liquid crystalline polymer (TLCP), a copolyester of HBA and PET with a composition of 80/20 mole ratio of HBA/PET, trade name Rodrun LC5000, purchased from Unitika Co., Japan. Above the melting temperature of 280 °C, it exhibits a liquid crystal phase. Its room temperature density is 1.41 g cm^{-3}. All materials were dried in a vacuum oven at 80 °C for 10 h before use.

2.2. Blending and film fabrication

PP was melt blended with various amounts of TLCP; 5, 10, 15, 20, 30 and 50 wt%. The blending was carried out using a co-rotating, intermeshing, twin-screw extruder (PRISM-TSE-16TC) with a screw diameter of 16 mm, length-to-diameter (*L*/*D*) of 25, at a fixed screw speed of 150 rpm. The processing temperature profile was 240/280/280/285/290 °C, representing the temperatures at the hopper zone, the three barrel zones, and the die head, respectively. The extruded strand was immediately quenched in a water bath, pelletized and vacuum dried at 80 °C for at least 8 h for the removal of moisture. The neat PP and the blends were then fabricated as extruded films using a mini-extruder (Randcastle RCP-0625) equipped with a cast film line. The screw speed used was 70 rpm and the temperature profile was 245/280/290/295 °C, for the hopper zone, two barrel zones and slit die zone, respectively. The gap at the die lip and the width were fixed at 0.65 and 152 mm, respectively. The film exiting from the die outlet was drawn and immediately cooled using a chilled roll. The film with a draw ratio of 30 (a die gap to film thickness), corresponding to the film thickness of about 20–25 μm, was prepared and used through out this work. If the content of TLCP was beyond 15 wt%, the film showed a rough surface due to the melt fracture.

2.3. Rheological measurements

Pellets of all blends including neat PP were pressed using a compression molding machine at 200 °C to get approximately 1-mm thick sheets. For neat TLCP, it was pressed at 290 °C. The polymer sheet was cut into disk of 20-mm diameter. The rheological measurements were performed at a fixed temperature of 295 °C (which was equal to the die temperature at the mini-extruder) on a plate–plate rheometer (Haake, Rotovisco RT20) with oscillation mode over the angular frequency range of 0.6–200 rad/s. The complex viscosity (η^*) was calculated from the dynamic storage modulus (G') and loss modulus (G''), defined by

$$\eta^* = \sqrt{\left(\frac{G'}{\omega}\right)^2 + \left(\frac{G''}{\omega}\right)^2},$$

where ω is the angular frequency.

2.4. Morphology

The blend extruded strands were cryogenically fractured in liquid nitrogen in order to reveal the geometry and distribution of TLCP dispersed phase in the strands. A thin layer of palladium was coated on the specimens using Hitachi E102 ion sputtering coater. The observation of the fractured strands was performed on a scanning electron microscope (SEM, Hitachi S2500) operated at 15 kV. To investigate the characteristic of TLCP fibers distributed in the composite films, the surface of the film was etched for 50 min in a permanganic etching solution (1% w/v) potassium permanganate in 4:4:10 part of water, phosphoric and sulphuric acid). After that, the mixture of 1:9 parts of hydrogen peroxide and water was poured into the etching solution to stop the reaction. Then the film was washed with distilled water. The etched film was dried and coated with gold platinum by EmScope SC500 coater using argon gas for sputtering. The SEM micrographs of the etched films were taken using SEM (Philips 515) operated at 12 kV.

2.5. Wide-angle X-ray scattering

In order to get the appropriate X-ray scattering intensity, a thick film (about 0.6–0.9 mm thick) was prepared by folding several layers of the thin film, while maintaining its relative MD direction. The X-ray scattering experiment was performed at room temperature on a three circle-transmission diffractometer (Philips PW1730/10) equipped with a copper target tube and operated at 40 kV and 40 mA. The diffractometer was operated in a symmetrical mode using a scintillation detector. The scattered intensities were recorded as a function of scattering vector, $|Q|$, varied from 0.2 to 6.0 Å^{-1} in steps of $\Delta|Q| = 0.02$ Å^{-1} and as a function of azimuthal angle, α, varied from 0 to 90° in steps of $\Delta\alpha = 9°$ with a count time of 10 s at each position. $|Q|$ is defined as $4\pi \sin\theta/\lambda$, where 2θ is the angle between the incident and scattered beam and λ is the incident wavelength of Cu Kα radiation (1.54178 nm).

2.6. Tensile testing

All films were cut into dumbbell-shape specimens (25 mm × 4 mm) using a punching machine. Tensile test was performed on a tensile tester (Instron model 4301). The crosshead speed of 50 mm/min was used with a full scale load cell of 10 N and a gauge length of 25 mm. For each sample, an averaged value of at least 10 measurements was determined in both MD and TD. All data were collected and analyzed using a package program 'Instron Series IX'.

3. Results and discussion

3.1. Rheological behavior

The complex viscosities of the neat components and the blends at various compositions, measured at 295 °C, are presented in Fig. 1. All specimens exhibit the shear thinning behavior, i.e. the viscosity decreases with increasing angular frequency or shear rate due to the induced chain orientation and resulting in a reduction of the entanglement density [23]. The viscosity of the neat PP is about 33–14 times higher than that of the neat TLCP over the frequency ranged from 0.6 to 200 rad/s, respectively. It is found that incorporation of 5 and 10 wt% TLCP into PP matrix causes a marked drop in the complex viscosity. With further addition of TLCP up to 50 wt%, the blend viscosity further decreases but to a less extent. This suggests that a small amount of TLCP added into the PP matrix can act as a processing aid or lubricating agent as reported earlier for the other TLCP/TP blend systems [5,6].

In general, the viscosity ratio ($\eta_{\text{dispersed phase}}/\eta_{\text{matrix}}$) plays an important rule on the morphology of the immiscible blend. To obtain good fibrillation in TLCP/TP blend, the viscosity ratio should be less than one [10]. Heino et al. [8] reported that the optimal viscosity ratio to obtain good fibrillation in Vectra A/PP and LC3000/PP blend systems prepared as extruded strands was in the range 0.5–1. However, our previous reports on LC3000/PP and LC3000/PE in situ composite films [14,24] fabricated by using a two-step method as employed in this work revealed that the viscosity ratio in the range as low as 0.02–0.15 was possible to generate fibrillar structure in the extruded films. This was due to the efficient extension at the step of film extrusion.

The viscosity ratio of LC5000/PP system, $\eta^*_{\text{LC5000}}/\eta^*_{\text{PP}}$ plotted as a function of frequency is illustrated in Fig. 2. The viscosity ratios are in the range 0.03–0.07 over the entire frequency region being investigated. These values are quite

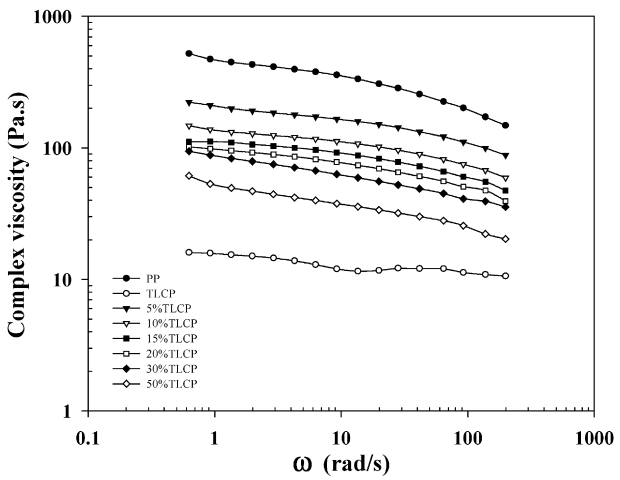

Fig. 1. Complex viscosities of PP, TLCP and their blends containing various TLCP contents, measured at 295 °C.

low and are within the same range as previously reported for the blends of PP or PE with LC3000. It is found that the viscosity ratio slightly increases with increasing frequency due to the faster drop of the viscosity of PP than that of TLCP in the high frequency range. Since the degree of entanglement for flexible molecules like PP is normally higher than that for the simi-rigid TLCP molecules, the reduction in the degree of entanglement in PP phase at high shear rate is therefore more pronounced.

3.2. Morphology

Fig. 3 shows SEM micrographs of the cryogenically fractured strands of in situ composites containing (a) 5, (b) 10, (c) 15, (d) 20, (e) 30 and (f) 50 wt% TLCP. All micrographs exhibit a two-phase system showing TLCP dispersed in PP matrix. It is clearly seen that the dispersed TLCP domains in 5 and 10 wt% TLCP/PP strands are mostly appeared in the form of droplets. Some elongated TLCP domains are seen in the strands of 15 and 20 wt% TLCP/PP. Long TLCP fibers with bigger diameters are observed in the specimen with 30 wt% TLCP. For 50 wt% TLCP/PP blend, a coarse phase separation took place. Large TLCP domains are seen with inner structure and gaps between them, showing a lack of connectivity in the matrix phase. The average diameters of TLCP domains are approximately 5, 8, 9, 10, 13 and 50 μm for the blends containing 5, 10, 15, 20, 30 and 50 wt% TLCP, respectively. The size of the TLCP dispersed phase in the extruded strands grows with increasing TLCP content, which is attributed to the higher possibility of the dispersed droplets to coalesce.

Fig. 4 shows the SEM micrographs of the etched composite films containing (a) 5, (b) 10 and (c) 15 wt% TLCP. These are presented in two columns; at a low magnification (× 143) in column I in order to present a wide view of fiber distribution and at a high magnification (× 573) in column II in order to see the shape and surface of TLCP fibrils. From column I, it is evident that the fibril length and the number of fibrils per unit area in the composite films increase with increasing TLCP content. From column II, it is seen that TLCP fibers are somewhat flatten due to the extrusion through a narrow slit die, and some fibers have very sharp tips which may arise from the necking of fibers followed by break-up after subjected to a high extension. The widths of TLCP fibers in all films shown in column II are approximately the same, i.e. in the range 5–10 μm. For each blend composition, the lengths of TLCP fibers in the film vary greatly (see Fig. 4, column I). Therefore, distribution of TLCP fiber aspect ratios (length to width) determined from about one hundred fibers are shown in Fig. 5 for the films containing 5 and 10 wt% TLCP. It is seen that the distribution profile becomes broader and shifts towards higher values when TLCP concentration is increased. Distribution of fiber aspect ratio for the film containing 15 wt% TLCP is not shown here because some very long fibers ended outside the viewing area. However, its distribution is expected to be even broader than that of the 10 wt% TLCP film.

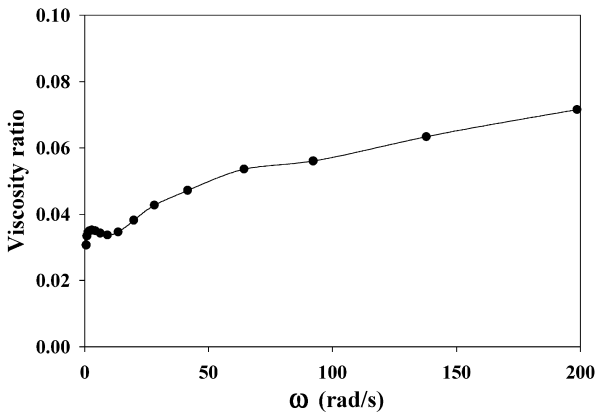

Fig. 2. Viscosity ratio (η_{TLCP}/η_{PP}) versus frequency at 295 °C.

3.3. Wide-angle X-ray scattering

The two-dimensional X-ray scattering patterns of the neat PP film and 5, 10 and 15 wt% TLCP composite films are shown in Fig. 6a–d, respectively. The vertical axis (meridional section) of the pattern corresponds to the machine direction (MD) of extruded films. The neat PP film (Fig. 6a) presents the diffused halo pattern with three main peaks at the scattering vector, $|Q|$, values of 1.05, 1.50, and 3.00 $Å^{-1}$, indicating no orientation. The three main peaks at the same positions as in the neat PP film are also observed in the scattering patterns of the composite films (Fig. 6b–d) but with variations in the intensity at the $|Q|$ values of 1.50 and 3.00 $Å^{-1}$. In particular, the arc-like patterns at $|Q| = 1.5$ $Å^{-1}$ on the equatorial section are clearly seen in the scattering patterns of the composites. The arc-like characteristics reduce to a more intense region with increasing TLCP content, implying that the higher orientation in the MD is achieved.

Fig. 7a compares the equatorial scans for the neat PP film, and the composite films comprising 5, 10 and 15 wt% TLCP. For all scans, there are three peaks appeared at $|Q| = 1.05$, 1.50 and 3.00 $Å^{-1}$, and a small shoulder at $|Q| \sim 2.00$ $Å^{-1}$. On examination of these scattering patterns, it is clearly seen that the peak intensity at $|Q| = 1.50$ $Å^{-1}$ increases with increasing TLCP content. This indicates that the major contribution of this peak intensity is from TLCP component. Thus to qualify the anisotropy of these samples, the azimuthal (α) scans at $|Q| = 1.50$ $Å^{-1}$ were run over 360°. The results are shown in Fig. 7b. The increase in the peak intensities imply that the level of anisotropy of the composite films is increased with increasing TLCP content, which is in accord with their 2-D scattering patterns (Fig. 6b–d). However, the azimuthal scan of neat PP film shows no peak, suggesting that the PP film is isotropic.

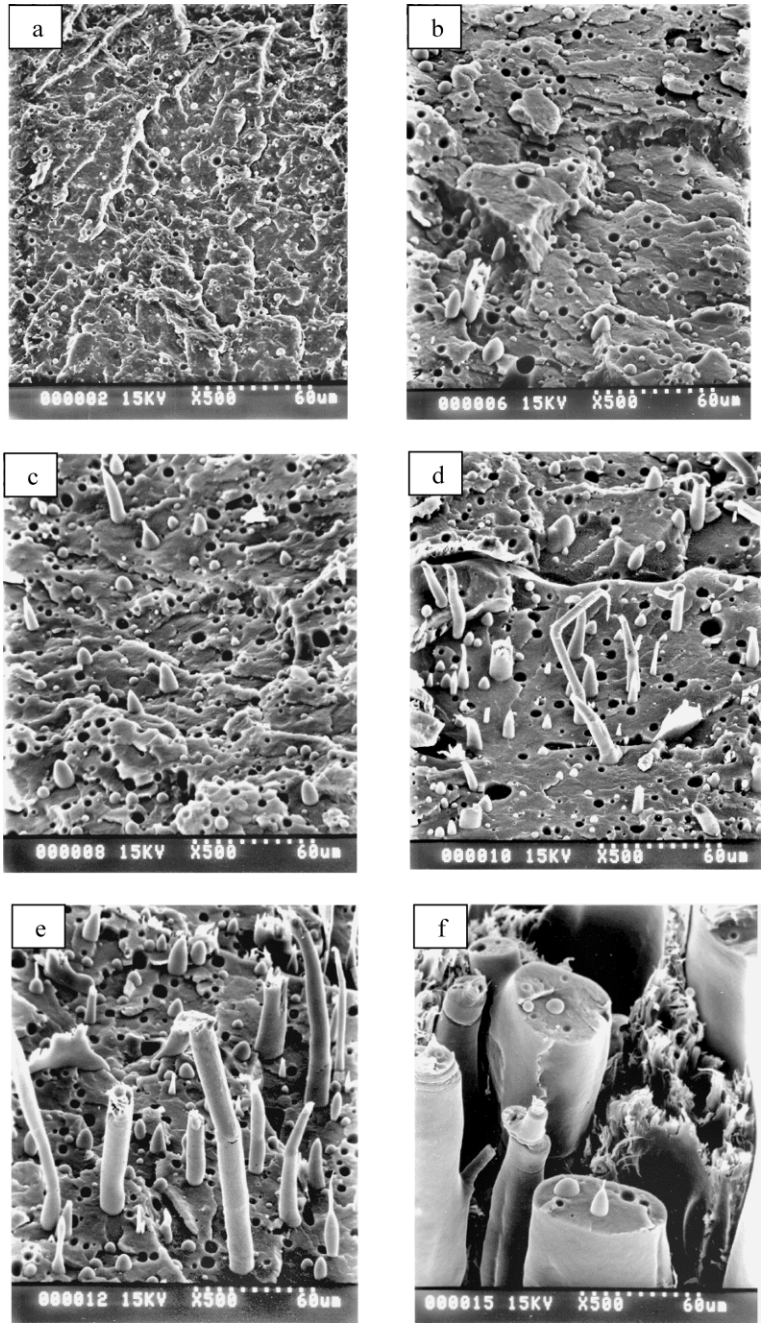

Fig. 3. SEM micrographs of cryogenic TLCP/PP strands at various TLCP contents: (a) 5, (b) 10, (c) 15, (d) 20, (e) 30 and (f) 50 wt%.

Furthermore, we have also quantified the order parameter, $\langle P_2 \rangle$, of the TLCP domain in the composite films from X-ray data by using a novel separation technique. The more details dealing with calculation of order parameters are presented in separate papers [25–27]. The order parameters for the TLCP phase in 5, 10 and 15 wt% TLCP/PP composite films are found to be 0.65, 0.75 and 0.76, respectively. The increase in the order parameter with increasing TLCP content corresponds to the enhancement of molecular orientation in TLCP phase.

3.4. Mechanical properties

Mechanical properties of neat PP and in situ composite films tested in both machine (MD) and transverse directions (TD) are presented in Table 1. Properties of neat TLCP film is not presented because it cannot be prepared by using the condition described in this work due to its very low melt strength. From Table 1, it is seen that Young's modulus in MD of the composite films increases significantly with increasing TLCP content, while the TD modulus only slightly increases, due to the uniaxial orientation of TLCP

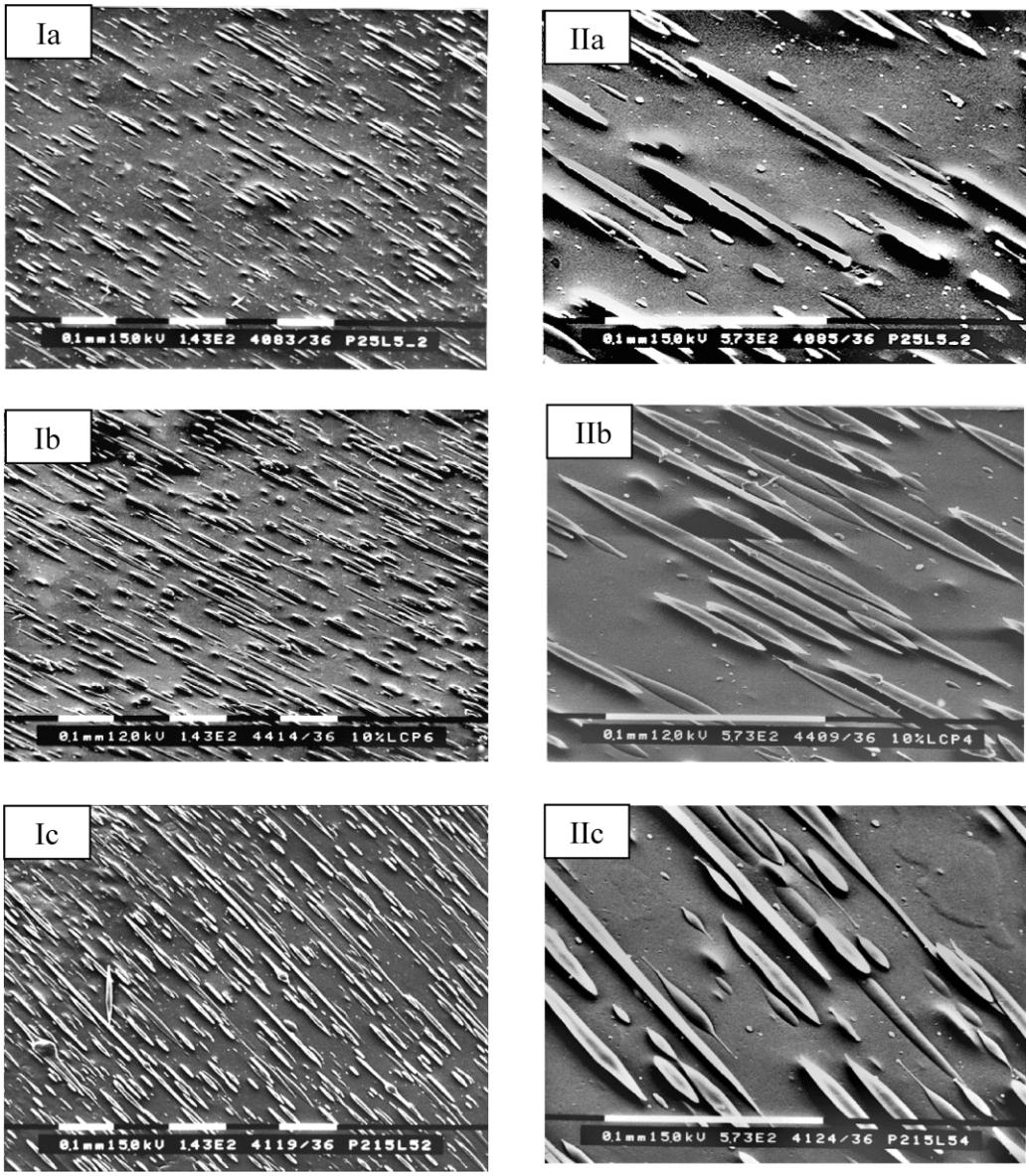

Fig. 4. SEM micrographs taken at magnifications of × 143 (column I) and × 573 (column II) for the etched TLCP/PP composite films containing: (a) 5, (b) 10 and (c) 15 wt% TLCP.

Table 1
The tensile properties of TLCP/PP composite films measured in machine (MD) and transverse directions (TD)

TLCP/PP (wt ratio)	Young's modulus (MPa)		Tensile strength (MPa)		Elongation at break (%)	
	MD	TD	MD	TD	MD	TD
0/100	743(59)	669(96)	42.9(4.0)	31.4(4.6)	660(47)	761(92)
5/95	945(56)	822(100)	39.8(1.6)	28.2(2.9)	836(27)	760(35)
10/90	1183(54)	672(54)	23.5(3.8)	21.1(3.3)	583(55)	727(77)
15/85	1706(118)	794(53)	25.1(4.4)	18.1(4.9)	509(55)	532(54)

Note: Numbers in the parentheses represent the values of standard deviation.

fibrils. Therefore the anisotropy in modulus progressively increases with addition of TLCP. Comparison of the MD modulus of the composite films with that of the neat PP film shows that the moduli of the composite films containing 5, 10 and 15 wt% TLCP are about 30, 60 and 130%, respectively, higher than that of the neat PP film. The increase in MD Young's modulus of the composite is attributed to three factors: (1) the increase in the number of the elongated fibers, (2) the increase of fiber aspect ratio (as seen in SEM micrographs of etched films shown in Fig. 4) and (3) the enhancement of molecular orientation in TLCP fibrils (as evident from WAXS). Enhancement of the order parameter suggests the increase in the intrinsic strength of TLCP fibrils, hence the effectiveness of reinforcement is increased. The tensile strengths in both MD and TD show a marked reduction with increasing TLCP content, suggesting

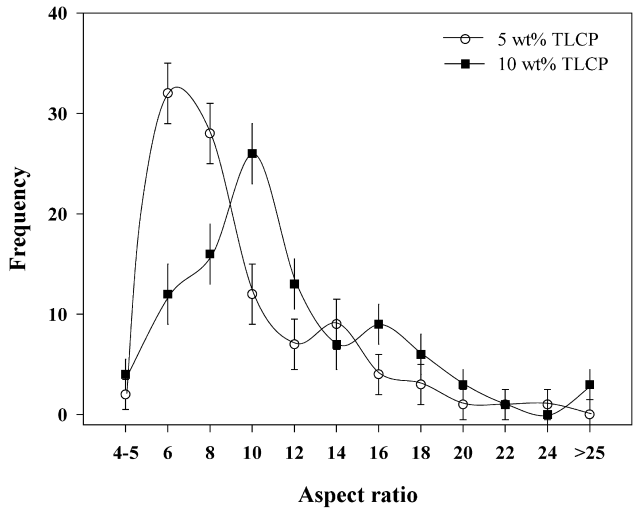

Fig. 5. Plot of the distribution curves between frequency and the fiber aspect ratio for the 5 and 10 wt% TLCP/PP composite films. The error bars reflect both sampling and measurement uncertainties.

that the interaction at fiber–matrix interfaces is poor, which is generally observed in the case of immiscible blends [3,4,28]. The values of elongation at break in both directions are slightly decreased with addition of TLCP. In most cases, the mechanical properties of in situ composites depend strongly on the amount of added TLCP, the degree of fibrillation and fiber orientation, including the level of molecular orientation [14,29,30].

The correlation between the fiber aspect ratio and Young's modulus is now examined. Since the values of the fiber aspect ratio are broadly distributed, we propose to use two types of the average values for evaluation of this

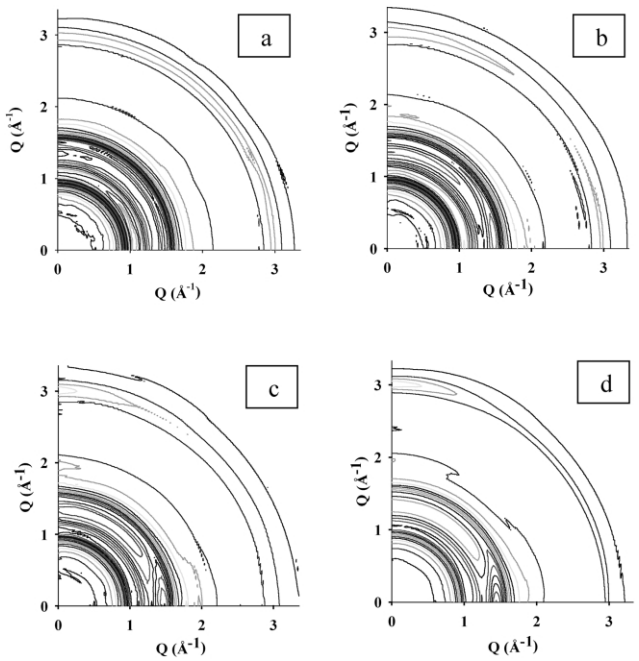

Fig. 6. The two dimensional X- ray scattering patterns for TLCP/PP composite films containing: (a) 0, (b) 5, (c) 10 and (d) 15 wt% TLCP.

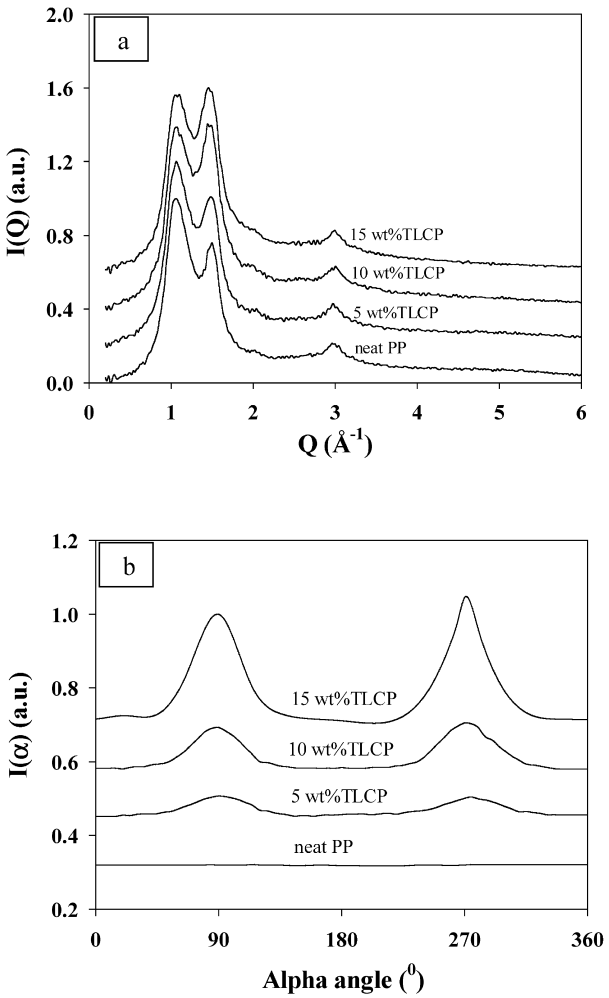

Fig. 7. (a) The equatorial X-ray scattering intensities, $I(Q)$ and (b) Azimuthal (α) scans at $Q = 1.50$ Å^{-1} for the neat PP film and the 5, 10 and 15 wt% TLCP/PP composite films.

correlation, i.e. the number average aspect ratio, $\langle l/d\rangle_n$, and the length-weighted average aspect ratio, $\langle l/d\rangle_l$, defined by the following equations:

$$\left\langle \frac{l}{d} \right\rangle_n = \frac{\sum_1^n (l_i/d_i)}{n} \tag{1}$$

$$\left\langle \frac{l}{d} \right\rangle_l = \frac{\sum_1^n l_i(l_i/d_i)}{\sum_1^n l_i} \tag{2}$$

where l_i is the length of the ith fiber, d_i is the width of the ith fiber, and n is the total number of fibers being evaluated.

Listed in Table 2 are the values of $\langle l/d\rangle_n$, $\langle l/d\rangle_l$, MD Young's modulus and the order parameter, $\langle P_2\rangle$, for the composite films containing 5, 10 and 15 wt% TLCP. Fig. 8 illustrates the plots of number average and length-weighted average aspect ratios against MD Young's modulus for comparison. It is seen that the plot of length-weighted

Table 2
Correlation between MD Young's modulus, order parameter $\langle P_2 \rangle$, the number average aspect ratio, $\langle l/d \rangle_n$, and length-weighted average aspect ratio, $\langle l/d \rangle_l$, of the TLCP/PP composite films at various compositions

TLCP/PP (wt ratio)	$\langle l/d \rangle_n$	$\langle l/d \rangle_l$	MD Young's modulus (MPa)	$\langle P_2 \rangle$
5/95	10.2	11.1	945	0.65
10/90	12.5	14.2	1183	0.75
15/85	12.9	21.0	1706	0.76

average aspect ratio versus MD modulus shows a linear correlation whereas the plot of number average aspect ratio versus MD modulus shows a linear relationship only in the low concentration range of TLCP (up to 10 wt%). This clearly indicates that the length-weighted average fiber aspect ratio is a more appropriate parameter to correlate with MD modulus since the long fibers are more effective than the shorter ones in the mechanism of reinforcement. On examination of the values of the order parameters and the MD moduli of the composites at various compositions (Table 2), it is seen that they are not linearly correlated. The values of order parameter for the 10 and 15 wt% TLCP films are approximately the same, whereas the MD modulus of 15 wt% TLCP film is much higher than that of the 10 wt% TLCP film. Therefore the effect of fiber aspect ratio seems to be more pronounced than the effect of molecular orientation in TLCP phase, in particular, when the fiber aspect ratio is high.

The well-known Tsai–Halpin equation [4,31] is often used to predict the longitudinal modulus of the composite (E_c) for the short fiber-filled composite systems. In this equation, E_c is related to the fiber modulus (E_f) and matrix modulus (E_m) of the uniaxially oriented composite materials reinforced with fibers of uniform aspect ratio. In addition, the stress and strain are assumed to be continuous along the interface. The Tsai–Halpin equation is expressed as:

$$\frac{E_c}{E_m} = \frac{(1 + ABX)}{(1 - BX)} \tag{3}$$

where X is the fiber volume fraction and

$$B = \left[\frac{E_f}{E_m} - 1 \right] / \left[\frac{E_f}{E_m} + A \right] \tag{4}$$

The quantity A is equal to $2(l/d)$. The theoretical E_c values are calculated by using the number average aspect ratio, $\langle l/d \rangle_n$, and E_f of LC5000 phase is assumed to be 65 GPa as determined by Nakamae et al. [32] for LC5000 sheet using X-ray technique. E_m equals 743 MPa for the MD modulus of neat PP film determined in this work. The comparison between the composite moduli calculated by using Eq. (3) with the measured values is presented in Fig. 9. The calculated values of E_c are 1.16, 1.74 and 2.38 GPa for 5, 10 and 15 wt% TLCP/PP films, respectively, which are about 23, 47 and 40% higher than those of the corresponding experimental values. The possible reasons for explanation of the lower measured values for the composite MD Young's moduli are; (1) poor interfacial adhesion at the interface of the immiscible blend makes the transmission of the stress from the matrix to the fiber less effective and (2) the fiber aspect ratio in the real system is not uniform as assumed in the theory, especially those with small value of aspect ratio greatly reduce the efficiency of reinforcement. It should be borne in mind that the Tsai–Halpin equation is essentially semi-empirical in origin and the extension of it to these in situ composites containing highly anisotropic fibrils may be inappropriate.

4. Conclusions

In the present study, we have investigated the rheology of the blends of PP and TLCP (Rodrun LC5000). The shear

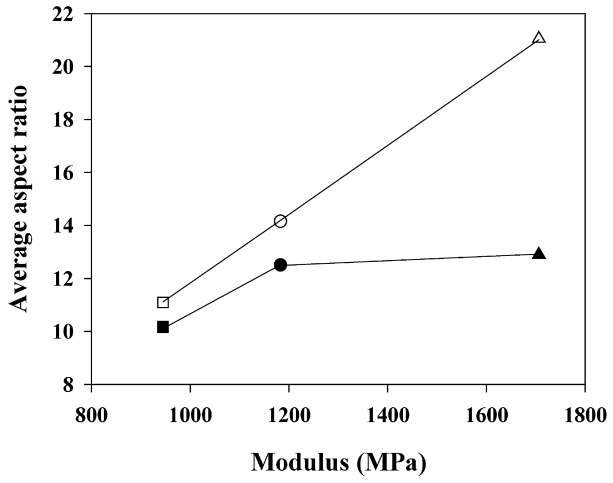

Fig. 8. Plots of the number average (filled symbol) and length-weighted average (opened symbol) fiber aspect ratio against MD Young's modulus for the 5 (■), 10 (●) and 15 (▲) wt% TLCP/PP composite films.

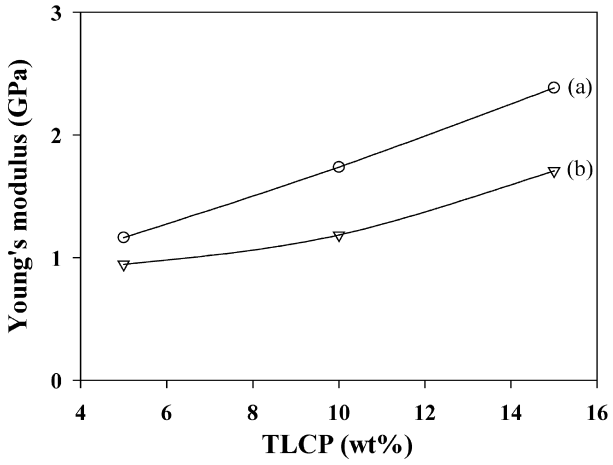

Fig. 9. MD Young's moduli of TLCP/PP composite films versus TLCP content: (a) predicted by Tsai–Halpin equation and (b) experimental results.

thinning behavior in the frequency range 0.6–200 rad/s is observed for all neat components and blends containing upto 50 wt% TLCP. The blend viscosity is found to decrease with increasing TLCP content, especially a marked drop in viscosity is observed in the blend with 5 wt% TLCP.

Morphology of the blend extruded strands containing $\leq$10 wt% TLCP reveals TLCP droplets. Some elongated TLCP domains are seen in 15 and 20 wt% TLCP/PP, long TLCP fiber with pull-out feature appeared in 30 wt% TLCP/PP and a coarse phase separation occurred in the case of 50 wt% TLCP/PP. The diameters of the TLCP droplets and fibers increase with increasing TLCP content, i.e. from about 5 to 50 μm.

The blends with 5, 10 and 15 wt% TLCP can be prepared as cast films with smooth surface at the draw ratio of 30 (about 20 μm thick). The number as well as the length of TLCP fibrils in the films increases with increasing TLCP content. As a result, MD moduli of the composite films are found to rise progressively with increasing TLCP concentration. The MD Young's moduli for the 5, 10 and 15 wt% TLCP/PP films are about 30, 60 and 130% higher than that of the neat PP film, respectively. A linear correlation between the length-weighted average fiber aspect ratio and MD modulus is observed.

Orientation function of TLCP domains is found to increase with TLCP content up to 10 wt%, beyond which it tends to level off at a value of 0.76. Moreover, the measured composite moduli are found to be about 23–47% lower than those predicted by Tsai–Halpin equation.

Acknowledgements

This work was granted by the Royal Golden Jubilee Program, the Thailand Research Fund, (grant number: PHD/00047/2541). The authors also would like to thank the Postgraduate Education for Research program in Chemistry (PERCH) for a partial support. And finally, we are also indebted to the Alexander von Humboldt Foundation for the donation of the rheometer.

References

[1] Kiss G. Polym Sci Engng 1987;27(6):410–23.
[2] Blizard KG, Baird DG. Polym Engng Sci 1987;27(9):653–62.
[3] Datta D, Fruitwala H, Kohli A, Weiss RA. Polym Sci Engng 1990;30:1005–18.
[4] Handlos AA, Baird DGB. JMS Rev Macromol Chem Phys 1995;C35(2):183–238.
[5] Mantia FPL, Paci VM, Magagnini PI. Polym Engng Sci 1990;30(1):7–12.
[6] Meng YZ, Tjong SC, Hay AS. Polymer 1998;39(10):1845–50.
[7] Wu S. Polym Engng Sci 1987;27(5):335–43.
[8] Heino MT, Hietaoja PT, Seppala JV. J Appl Polym Sci 1994;51:259–70.
[9] Jin X, Li W. JMS Rev Macromol Chem Phys 1995;C35(1):1–13.
[10] Taylor GI. Proc Roy Soc 1934;A146:501–23.
[11] He J, Bu W, Zhang H. Polym Engng Sci 1995;35(21):1695–704.
[12] Wanno B, Samran J, Bualek-Limcharoen S. Reol Acta 2000;39:311–9.
[13] Bastida S, Eguiazabal JI, Nazabal J. Polymer 2001;42:1157–65.
[14] Nakinpong T, Bualek-Limcharoen S, Bhutton A, Aungsupravate O, Amornsakchai T. J Appl Polym Sci 2002;84:561–7.
[15] Hull JB, Jones AR. In: Arcierno D, Collyer AA, editors. Rheology and processing of liquid crystalline polymers. London: Chapman and Hall; 1996. p. 218.
[16] Jones FR. Handbook of polymer–fiber composites. Essex: Longman Scientific and Technical; 1994. pp. 279.
[17] Crevecoeur G, Groeninckx G. Polym Engng Sci 1993;33:532–42.
[18] Hsu TC, Lichkus AM, Harrison IR. Polym Engng Sci 1993;33(13):860–3.
[19] Chunsirikul W, Hsu TC, Harrison IR. Polym Engng Sci 1996;36(22):2708–17.
[20] Qin Y, Brydon DL, Mather RR, Wardman RH. Polymer 1993;34(17):3597–608.
[21] Xu QW, Man HC, Lau WS. Comp Sci Tech 1999;59:291–6.
[22] Sukananta P, Bualek-Limcharoen S, J Appl Polym Sci.
[23] Nielsen LE. Polymer rheology. New York: Marcel Dekker; 1977. p. 47–51.
[24] Bualek-Limcharoen S, Saengsuwan S, Amornsakchai T, Wanno B. Macromol Sym 2001;170:189–96.
[25] Mitchell GR, Saengsuwan S, Bualek-Limcharoen S. Polymer Preprint 2002;43(1):197–8.
[26] Mitchell GR, Saengsuwan S, Bualek-Limcharoen S, submitted to J Appl Crystallogr.
[27] Saengsuwan S, Mitchell GR, Bualek-Limcharoen S, submitted to Polymer.
[28] Nielsen LE. Mechanical properties of polymers and composites, II. New York: Marcel Dekker; 1974.
[29] Ajji A, Brisson J, Qu Y. J Polym Sci (B) 1992;30:505–16.
[30] Lin Q, Jho J, Yee AF. Polym Engng Sci 1993;33(13):789–98.
[31] Halpin JC, Kardos JL. Polym Engng Sci 1976;16(5):344–52.
[32] Nakamae K, Nishino T, Kuroki T. Polymer 1995;36(14):2681–4.